The HKU Scholars Hub The University of Hong Kong 香港大學學術庫

Title	Measuring asymmetries of skin lesions
Author(s)	Ng, Vincent; Cheung, David
Citation	Proceedings Of The Ieee International Conference On Systems, Man And Cybernetics, 1997, v. 5, p. 4211-4216
Issued Date	1997
URL	http://hdl.handle.net/10722/45574
Rights	©1997 IEEE. Personal use of this material is permitted. However, permission to reprint/republish this material for advertising or promotional purposes or for creating new collective works for resale or redistribution to servers or lists, or to reuse any copyrighted component of this work in other works must be obtained from the IEEE.

Measuring Asymmetries of Skin Lesions

Vincent Ng

Department of Computing, Hong Kong Polytechnic University, Kowloon, Hong Kong

David Cheung

Computer Science Department, University of Hong Kong, Hong Kong

ABSTRACT

Since 1994, a clinical study has been established to digitize melanocytic lesions from patients who are referred to the Colored Pigment Lesion Clinic in the University of British Columbia. In the past, we have been using circularity as the main feature to reflect the asymmetrical aspect of skin lesions. However, its significance often depends on the accuracy of image segmentation while the borders of many lesions are often fuzzy and irregular. In this paper, we investigate how to use symmetry distance (SD) to improve the measurement of the asymmetries of skin lesions. Two SDs, including the basic SD and the fuzzy SD, and the simple circularity are calculated based on the new set of color images which are digitized under the controlled environment.

Keywords: circularity, symmetry distances, melanomas, medical imaging

1 Introduction

Malignant melanoma is the most common cancer in people less than 35 years of age and incident rates are increasing by approximately 5% per annum in many white populations, including British Columbia, Canada [1]. Without timely diagnosis and treatment, it is frequently fatal. However, the prognosis for cure is excellent when the malignant melanoma is detected early and removed by surgery [2]. In recent years, with increasing public awareness of the disease and the importance of early detection, more and more people are seeking professional advice for pigmented lesions. Skin biopsies have become the most reimbursed Medicare procedure in the USA [3]. Early identification reduces the risk of death from melanoma but a false positive diagnosis adds extra cost to health care, and also causes unnecessary surgery for patients. There are guidelines developed to recognize dysplastic nevi and malignant melanomas such as the ABCD rule [2] and the Seven-point Checklist [4]. However, diagnosis of some of the lesions is difficult even for the trained dermatologists. It is highly desirable to develop clinical tools to aid the diagnosis. Different approaches have been used by many researchers to improve clinical diagnosis accuracy. The journal *Computerized Medical Imaging and Graphics* devoted the 1992 May/June issue to discuss some of the techniques. Other publications include measuring the infrared and ultraviolet reflectance [5], utilizing a low-power surface microscope [6], digitizing and analyzing the pre-existing slides [7], and constructing a spectroanalyzer [8].

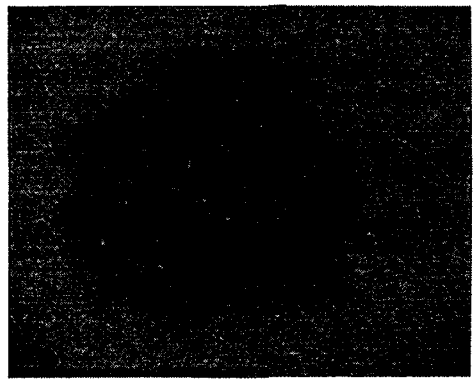

Figure 1: A Skin Lesion.

Since 1994, we have conducted a clinical study to digitize melanocytic lesions under a controlled environment for patients who are referred to the Pig-

The work of the first author was supported in part by the Polytechnic University Research Grant: 351/089.

0-7803-4053-1/97/$10.00 © 1997 IEEE

mented Lesion Clinic in the University of British Columbia, Canada. When reviewing the melanocytic lesions, they can be divided into 3 types; benign nevi, dysplastic nevi and malignant melanomas. Benign melanocytic nevi are usually less than 5 mm in diameter, with a regular or distinct border, and its color is orderly or tan-brown. Dysplastic nevi are greater than 5 mm and have borders that are usually irregular and frequently ill-defined. The color is variegated, ranging from tan to dark brown on a pink background. Malignant melanomas are characterized by sudden or continuous changes in size and the development of an irregular and/or notched border. In summary, there are four clinical criteria to diagnosis a lesion, namely shape, size, color and irregularity of the border. It is the first criterion which has raised our interest in applying the symmetry distance to provide a measure to discriminate different types of melanocytic lesions.

In a previous study, twelve different features with respect to the clinical guidelines for differentiating skin lesions, such as asymmetry, intensity and irregularity, were applied to a sample set of images of skin lesions. Two of them were found to be significant, namely circularity and fractal dimension [7].

In this paper, we investigate how to use symmetry distance (SD) to improve the measurement of the asymmetries of skin lesions. We improve the SD to deal with fuzzy borders of skin lesions as well as to reduce its computational complexity. Two SDs, including the basic SD and the fuzzy SD, and the simple circularity are calculated based on the new set of color images which are digitized under the controlled environment.

2 Images

The **RGB** color images with pixel resolution 512 x 486 are digitized by a hand-held camera which is placed directly on the patient's skin (see Figure 1). Around the edge of the camera, there is a ring of light providing a standard lighting condition. Each image has one or more lesions located near the centre and the lesions are surrounded by normal skin. Sometimes there are hairs, pigments and a bright blue ink mark (a marker made by the dermatologist). Usually, the intensity of the normal skin is uniformly distributed, but the lesion can vary in size, shape, color and intensity. In many cases, the separation between a lesion and the surrounding skin is fuzzy. After careful examining the images, some interesting characteristics are observed: lesions are usually darker or more red in color than the surrounding skin not because they have more red pigment, but because they are lacking in the blue component. Furthermore, the blue band shows a better separation for the lesions than the other two bands. Hence, we have developed a rule-based system to put more weight on the blue band during the segmentation step [9].

1. *Let P be a shape with n points.*
2. *Fold the points of P by rotating each point P_i counterclockwise about the centroid of P by $2\pi i/n$ radians.*
3. *Calculate the average of the points as P_0.*
4. *Unfold the points by duplicating P_0 and rotate clockwise about the centroid by $2\pi i/n$ radians.*

Figure 2: Symmetry Transform Algorithm.

3 Circularity

In many previous studies, *circularity* is used as the main feature to reflect the asymmetrical aspect of skin lesions [10, 11, 12]. However, its significance often depends on the accuracy of image segmentation while the borders of many lesions are often fuzzy and irregular. Its basic formula is

$$CIRC = \frac{4\pi A}{P^2} \tag{1}$$

where P and A are the perimeter and area, respectively. For a given perfect circle, $CIRC$ equals to 1. This measurement is independent of scale, as both denominator and numerator are proportional to the square of the perimeter for a given shape. However, the border of a lesion may be highly irregular and is similar to a fractal curve [13]. This would cause the segmented region of an image appeared to have a thick border but a small internal area. The calculated value of $CIRC$ will then become very small and does not reflect the correct measurement. One may try to apply thinning algorithms to reduce the unnecessary border points. Though this will not only add extra complexity in the analysis, but a simple thinning algorithm may fail to work correctly for a fractal border as well.

4 Symmetry Distance

In order to solve the problems of using circularity to model the asymmetry of skin lesions, we have

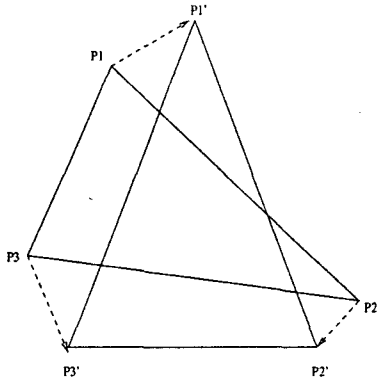

Figure 3: The distance between shapes P and Q.

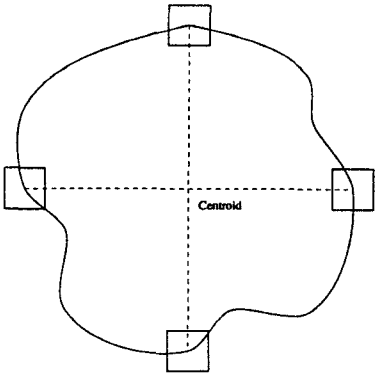

Figure 4: Selecting points at regular angular intervals.

adopted the use of *Symmetry Distance* (SD) [14]. Before defining the SD, we first describe what is the meaning of the *distance* between two given shapes. In Figure 3, shape P is made up of points P_1, P_2 and P_3, while shape Q is made up of points P_1', P_2' and P_3' respectively. The distance between the two shapes is the total displacement of moving the corresponing points from P to Q divided by three. Formally, for any two shapes with n points, P and Q, their distance is defined as

$$d(P,Q) = \frac{1}{n}\sum_{1}^{n} \|P_i - Q_i\|^2 \qquad (2)$$

For a shape P, the *symmetry transform* is a transformation that will convert P into a symmetric shape closest to it, and the resultant shape is represented as $ST(P)$. The SD of P is then the minimum distance required to move points from P to $ST(P)$. That is

$$SD = \frac{1}{n}\sum_{1}^{n} \|P_i - P_i'\|^2 \qquad (3)$$

where P_i and P_i' are points in P and $ST(P)$ respectively. Note that, similar to circularity, the definition of SD has implied invariance to rotation and translation. However, its use requires a geometrical algorithm to perform ST. The original ST algorithm from [14] is shown in Figure 2.

The algorithm has a folding step and an unfolding step. Its computational requirement is acceptable when there are only a relatively small number of points for a shape. It is becoming computationally expensive, though, when there can be hundreds of points on the border of a lesion. One possibility is to select a small set of points for the SD calculation. With this approach, the choice of points will influence the value of SD and depends on the actual shape of a lesion to be measured. One method is to consider selecting points by equal distance, but it may not be appropriate for fuzzy shapes. For example, in Figure 8, the border of the segmented lesion is highly irregular and many points on the border are clustered together. Equal distance selection may result with non-characteristics points to represent the actual shape of the lesion. Another method is to select points by using the smoothing procedures proposed in [14]. In this case, the SD calculation still requires the folding and unfolding steps. In order to eliminate these two steps, we suggest to select points at regular angular intervals with respect to the centroid. For example, in Figure 4, points at 0, $\frac{\pi}{2}$, π, and $\frac{3\pi}{2}$ with respect to the centroid are selected. However, the selected points may not be sufficient to represent the symmetrical behavior of the lesion. Therefore, we apply two techniques to remedy the problem in our new adaptive algorithm.

- We divide 2π by $m-1$ equal angular intervals. For each angle with respect to the centroid, we calculate a smoothed point from the set of points of a shape which has the same angular degree. Therefore, m smoothed points are created to represent the shape.

- SDs are iteratively calculated with an increasing number of smoothed points until the relative ratio between two successive SDs is lower than a preset tolerance.

The new algorithm is shown in Figure 5. As points are selected at regular angular intervals, the folding and unfolding steps in the *Symmetry Transform* are not necessary, and we can calculate the P_0 directly from the distances of the smoothed points to the cen-

1. *Calculate m smoothing points of P. The smoothed points are evenly distributed along the angular displacement with respect to the centroid.*
2. *Select k points at regular angular intervals to calculate the first SD.*
3. *While (relative ratio between successive SDs > a tolerance level)*
   - *Let $k = 2 \times k$.*
   - *Calculate the new SD.*

Figure 5: Adaptive SD Algorithm.

troid. In our work, we have experimented with different values for m and find that 90 is sufficient for most of our images. For the rest of the paper, we called the SDs calculated from the original algorithm in [14] as BSD and ASD for our modified adaptive algorithm.

5 Fuzzy Symmetry Distance

The previous SD calculations relied heavily on the segmentation result. For a malignant nevus (lesion), we would expect it to have a highly ill-defined border with which segmentation of the image can be difficult. We also observe that nevus images in general have a degree of randomness along the borders of lesions. To cope with the border fuzziness, there can be two approaches when calculating SDs. The first approach is to estimate the actual shape during the calculation of SDs. The second approach is to improve the discriminative power of the SDs by widening its numeric range for the images of lesions.

The first approach is similar to finding a better segmentation method, which is difficult. Furthermore, as we are not interested in the absolute values of SDs, but rather on the relative distributions between SDs of symmetrical and asymmetrical lesions, the second approach is more appealing. Suppose there is a simple shape R with its centroid as C, and a scalar factor f where $0 \leq f \leq 1$. After calculating its P_0, we can increase its SD by the following procedures.

- Move a point of R by the factor f inward when its distance from the centroid of R is less than that of P_0.
- Move a point of R by the factor f outward when its distance from the centroid of R is more than that of P_0.

1. *Let c be the centroid of P.*
2. *Calculate m smoothing points of P. The smoothed points are evenly distributed along the angular displacement with respect to the centroid.*
3. *Select k points at regular angular intervals.*
4. *While (relative ratio between successive SDs > a tolerance level)*
   - *Let Avgd be the average distance of the k points from the centroid.*
   - *For each point p*
     - *If ($\|p - c\| < Avgd$) then move p towards c with the fuzzy factor f;*
       Else move p away from c with the fuzzy factor f.
   - *Calculate the SD.*
   - *Let $k = k \times 2$.*

Figure 6: Fuzzy SD Algorithm.

The factor f above is used to represent the segmentation accuracy. We call this factor as the *fuzzy factor*. For a point P_i lying on the border of R, the fuzzy factor implies that the actual location of P_i can be any point within a circle whose centre is at P_i and radius is $\|P_i - C\| \times f$. With the fuzzy condition, we revised the Adaptive SD Algorithm to be the *Fuzzy SD Algorithm* as presented in Figure 6. To distinguish it from the others, we name the SDs calculated from it as FSD thereafter.

6 Results

To test the performance of the different symmetrical measurements, we used 84 images of melanocytic lesions which are not hairy in our image dataset. An example of a hairy image is shown in Figure 7. Each color image has three color bands (RGB) and each band has 256 levels. It is segmented by the multistage method [9] into two major regions: the nevus region and the non-nevus region. An example is shown in Figure 8 where the segmented lesion is surrounded by white lines.

For each lesion, a dermatologist has been asked to diagnosis it with the $ABCD$ criteria. If a lesion's image has been diagnosed with **A**, we label it as having an **asymmetry** problem. This information is used to compare the performance of the different symmetrical measurements.

After the segmentations, we transformed the color

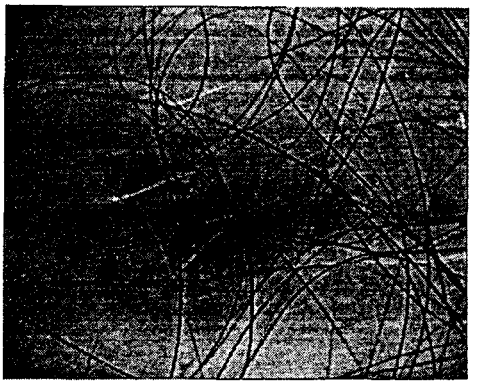

Figure 7: A Hairy Image.

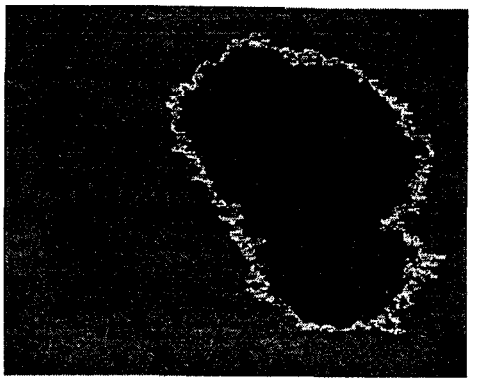

Figure 8: A Segmented Lesion.

images into gray level images by using the TIFF library. The gray level images are processed to compute their corresponding symmetrical measurements. Each image then has the 4 symmetrical measurements calculated. The student t-test is used to compare the mean values of the measurements between the symmetric and asymmetric lesions. The result is shown in Figure 9. The F-value at each row indicates the significance between the distribution of symmetrical measurements of the lesions of the corresponding method. If it is large, then the method has a better differentiating ability.

Among all the methods, the simple circularity, $CIRC$, still performed reasonably well. It has a F-value of 2.13 and the difference between the means is about 0.06. The BSD method has the worst differential ability; while the FSD has the best performance among all. It has a F-value of 2.56 and the difference between the means is about 0.15. During the calculations of the measurements, we observed that for lesions with irregular(fuzzy) borders, the values of circularity can be very high and failed to reflect the actual values that are intended to measure.

7 Conclusion

In this paper, we have been applying the symmetry distance in measuring the asymmetry of a lesion. We calculated the different symmetrical measurements for the color images digitized from lesions of patients visiting the Colored Pigment Lesion Clinic in Vancouver, Canada. From the results, we observed that the fuzzy SD performed best in gray level images. In order to improve our work, further investigation is needed. Some of them is shown below.

	Mean (Asymmetric)	Mean (Symmetric)	F-Value
$CIRC$	0.172	0.229	2.13
BSD	0.504	0.413	1.47
ASD	0.625	0.676	2.07
FSD	0.179	0.327	2.56

Figure 9: Symmetrical Measurements for the Gray Level Images

- Enhance the current segmentation algorithm for hairy images so as to include more images to validate the symmetrical measurements.
- Develop a better asymmetrical measure which will consider regional shapes of a complicated lesion.

References

[1] R.P. Gallagher, M.A. Becky, D.I. McLean, C.P. Yong, V. Ho, J.A. Carruthers, and L.M. Warshawski, "Trends in Based Cell Carcinoma, Squamous Cell Carcinoma, and Melanoma of Skin from 1973 through 1987", *J. of the American Academy of Dermatology*, Vol. 32, pp. 413-412, 1990.

[2] R.J. Friedman, D.S. Rigel and A.W. Kopf, "Early Detection of Malignant Melanoma: The Role of Physician Examination and Self-Examination of the Skin", *Cancer Journal for Clinicians*, Vol. 35, No. 3, pp. 130-151, May/June 1985.

[3] W.V. Steocker and R.H. Moss, "Editor: Digital Imaging in Dermatology", *Computerized Medical Imaging and Graphics*, Vol. 16, No. 3, pp. 145-150, 1992.

[4] M.F. Healsmith, J.F. Bourke, J.E. Osborne and R.A.C. Graham-Brown, "An Evaluation of the Revised Seven-point Checklist for the Early Diagnosis of Cutaneous Malignant Melanoma", *British Journal of Dermatology*, Vol. 130, pp. 48-50, 1994.

[5] R. Marshall, "Infrared and Ultraviolet Reflectance Measurements as an Aid to the Diagnosis of Pigmented Lesions of Skin", *J. of Audiovisual Media in Medicine*, Vol. 4, pp. 11-14, 1981.

[6] H.P. Soyer, J. Smolle, S. Hodl, et. al., "Surface Microscopy:a New Approach to the Diagnosis of Cutaneous Pigmented Tumors", *American Journal of Dematopath*, Vol. 11, pp. 1-10, 1989.

[7] V. Ng and A. Coldman, "Computerized Differentiation of Melanoma From Benign Pigmented Lesions", *The Third Annual Western Canadian Society of Clinical and Investigative Dermatology Symposium*, Jasper, Canada, Feb. 1992.

[8] H. Zeng, C. MacAulay, B. Palcic and D. McLean, "A Computerized Autofluorescence and Diffuse Reflectance Spectroanalyzer System for IN VIVO Skin Studies", *The Third Annual Western Canadian Society of Clinical and Investigative Dermatology Symposium*, Jasper, Canada, Feb. 1992.

[9] T. Lee, V. Ng, D. McLean, A. Coldman, R. Gallagher, and J. Sale. "A Multi-Stage Segmentation Method for Images of Skin Lesions", *Proc. of IEEE Pacific Rim Conference on Communications, Computers, and Signal Processing*, pp. 602-605, May 17-19, 1995, Victoria, Canada.

[10] L. Andreassi, R. Perotti, M. Burroni, G. Dell'Eva and M. Biagioli, "Computerized image analysis of pigmented lesions", *Chron. Derm.*, Vol. V, 1995, pp. 11-24.

[11] N. Cascinelli, M. Ferrario, R. Bufalino, S. Zurrida, V. Galimberti, L. Mascheroni, C. Bartoli and C. Clemente, "Results obtained by using a computerized image analysis system designed as an aid to diagnosis of cutaneous melanoma", *Melanoma Research*, Vol. 2, 1992, pp. 163-170.

[12] J.E. Golston, W.V. Stoeker, R.H. Moss and I.P.S. Dhillon, "Automatic Detection of Irregular Borders in Melanoma and Other Skin Tumors", *Computerized Medical Imaging and Graphics*, Vol. 16, No. 3, pp. 199-203, 1992.

[13] V. Ng and A.J. Coldman, "Diagnosis of Melanoma with Fractal Dimensions", *IEEE Region 10 International Conference on Computers, Communications, Control and Power Engineering*, Beijing, China, October 19-21, pp. 514-517, 1993.

[14] H. Zabrodsky, S. Peleg and D. Avnir, "Continuous symmetry measures", *J. Am. Chem. Soc.*, Vol. 114, pp. 7843-7851, September 1992.